Available online at www.sciencedirect.com
SCIENCE DIRECT®
Engineering Structures 27 (2005) 699–708
ENGINEERING STRUCTURES
www.elsevier.com/locate/engstruct

Parametric study and design of rib-reinforced steel moment connections

Cheng-Chih Chen*, Cheng-An Lu, Chun-Chou Lin

Department of Civil Engineering, National Chiao Tung University, 1001 Ta Hsueh Road, 30010 Hsinchu, Taiwan

Received 11 August 2004; received in revised form 10 November 2004; accepted 24 December 2004
Available online 24 February 2005

Abstract

Seismic behavior of moment connections used in moment-resisting frames can be improved by adding vertical ribs to beam-to-column joints. A parametric study is conducted here to investigate effects of design parameters of the rib on the connection behavior. Three geometrical parameters were set for the rib characterized with an extension. Moreover, nonlinear finite element analysis was used for the parametric analysis. The stress distribution and plastic strain demand for various combinations of these parameters are also presented and compared. The numerical results indicate that a single lengthened rib can eliminate the concentrations of stresses and strains found in the unreinforced connection, and reduce the potential for brittle fracture of the connection. On the basis of the numerical results and the confirmation of previous experiments, rib design variables are recommended, along with a design procedure.

Keywords: Rib reinforcement; Moment connection; Weld access hole

1. Introduction

The Northridge earthquake in 1994 significantly damaged steel moment-resisting frames, which are supposed to provide ductility in connections during large earthquakes. Numerous steel beam-to-column connections did not behave in a ductile manner, and failed to provide the expected inelastic deformation [1]. Since the Northridge earthquake, many studies have been undertaken to investigate the behavior of the moment connection. Numerous specimens have been tested to find ways of enhancing their ductility for use in future steel buildings. Several tests have displayed that connections with pre-Northridge details may fail at low plastic rotation [2–4]; in most cases those unreinforced connections fail to develop the plastic rotation of 3% rad required by the 1997 AISC seismic provisions [5]. The specimens typically failed owing to fracture of the beam flange and groove weld, caused by through-thickness cracking originating at the root of the weld access hole. However, tests performed by Ricles et al. [6] demonstrated that unreinforced connections can also develop significant inelastic behavior. Ricles et al. tested 11 welded unreinforced moment connections with a high toughness weld metal and modified details, including beam web attachment detail and weld access hole geometry. Generally, satisfactory plastic rotation can be achieved by strengthening the connection or weakening the beam section. Accordingly, several ductile-behaved moment connections were recommended as presented in the FEMA publication [7].

Among the various strengthening schemes, it is common to use vertical rib plates to improve the seismic performance of steel moment connections. Such ribs generally have the form of a tapered triangular plate. The ribs welded to the top and bottom beam flanges at the column face are used to reduce the stresses at the beam flange groove weld, and to move the critical section away from the column face. Popov and Tsai [8] tested three connections reinforced with two vertical ribs to each beam flange. One connection was attached to the column flange, while the other two were joined to the column web. The strong axis connection had only 1.46% rad of plastic rotation due to the failure of the bottom flange weld and the weld joining the rib to the column flange. However, two weak axis connections

* Corresponding author. Tel.: +886 3 571 2121x54915; fax: +886 3 572 7109.
E-mail address: chrischen@mail.nctu.edu.tw (C.-C. Chen).

0141-0296/$ - see front matter © 2005 Elsevier Ltd. All rights reserved.
doi:10.1016/j.engstruct.2004.12.007

Table 1
Summary of test specimens [11,12]

Specimen	Beam[a] (mm)	Column[a] (mm)	Rib plate thickness (mm)	Rib plate geometry $h_r \times L_r \times h_e$ (mm)
SRL20	H588 × 300 × 12 × 20	H550 × 550 × 30 × 40	20	125 × 800 × 20
SRL30	H588 × 300 × 12 × 20	H550 × 550 × 32 × 40	30	125 × 800 × 30
SRE6-1	H588 × 300 × 12 × 20	H550 × 550 × 30 × 40	18	110 × 680 × 20
SRE6-2	H588 × 300 × 12 × 20	H550 × 550 × 30 × 40	18	94 × 460 × 20
SRE7-1	H700 × 300 × 13 × 24	H550 × 550 × 36 × 40	22	93 × 700 × 20
SRE7-2	H700 × 300 × 13 × 24	H550 × 550 × 36 × 40	18	97 × 640 × 15

[a] Dimensions are shown for depth, width, web thickness, and flange thickness, respectively.

exhibited excellent ductile behavior, and no weld fractures occurred. Tests conducted by Engelhardt et al. [9] and Anderson and Duan [10] demonstrated that connections reinforced with tapered triangular ribs exhibited sufficient hysteretic behavior with plastic rotation ranging from 2.5% to 3.0% rad. Engelhardt et al. tested two connections reinforced with two tapered ribs welded to the top and bottom beam flanges. Gradual tearing of the beam bottom flange at the rib tips caused the connection failure. Anderson and Duan tested three connections using a single rib welded to each beam flange. Failure was caused primarily by cracking of the weld between the rib and the column flange. Chen et al. [4] tested two connections reinforced by a single triangular rib welded to the centerline of each beam flange. One connection failed owing to a brittle fracture in the beam flange at the rib tip, while the other displayed stable hysteretic behavior.

Chen et al. [11] proposed another rib type. A single lengthened rib is welded to the centerline of the top and bottom beam flanges to increase the rib effect. As revealed from the numerical and experimental studies [4], a single rib is more effective than double spaced ribs for reducing the localized stress concentration near the weld access hole, and decreasing the potential for fracture. The lengthened portion of the rib is an intentional design feature that prevents beam flange fracture at the rib tip. Previous experimental study, to be briefly presented in a subsequent section, has demonstrated that single lengthened rib-reinforced connections can sustain cyclic lateral force and provide sufficient ductility during the large deformation. This study investigates the effects of the geometrical parameters of the lengthened rib on the behavior of the rib-reinforced moment connection. Three-dimensional nonlinear finite element models are designed to study the stress and strain distributions at several critical sections of the connection. On the basis of the results of the parametric study and previous experiments, a design procedure is proposed for practical applications.

2. Previous experimental work

Experimental research has investigated the cyclic behavior of moment connections reinforced with lengthened flange rib [11,12]. Two specimens were tested in the pilot proof-test [11], and four specimens were further tested for the parametric study [12]. Table 1 tabulated the specimen dimensions and the geometry of the lengthened ribs. Various lengthened ribs were designed for corresponding beams. Fig. 1 presents a typical connection detail, and Fig. 2 illustrates the geometry of the lengthened rib. A single lengthened rib was welded to each beam flange in the plane of the beam web to prevent the fracture initiating in the weld access hole region. The rib comprises a main reinforced part, a curved part, and an extension. The main reinforced part of the rib is designed to reduce the demand on the full penetration groove weld joining the beam and column flanges. The rib extension is proposed to mitigate the potential stress concentration on the beam flange at the rib tip and consequent tearing of the beam flange.

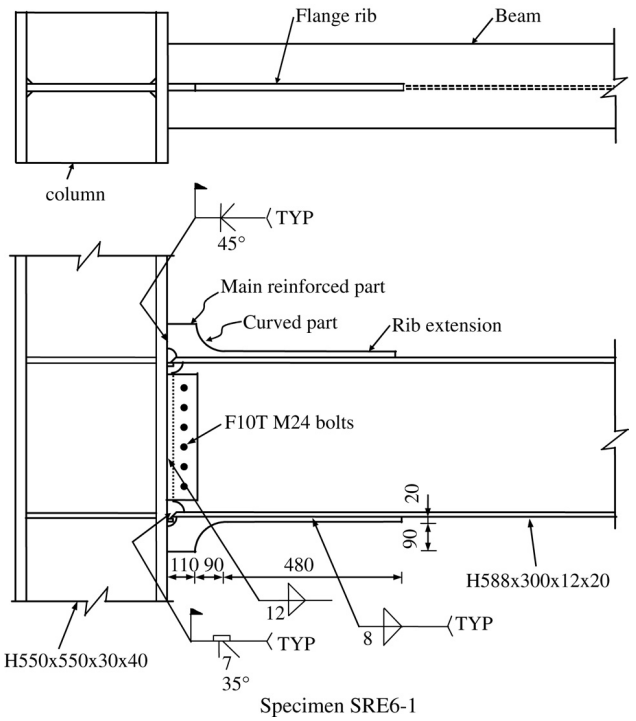

Fig. 1. Typical connection details [12].

Specimens represent an exterior beam-to-column connection; therefore, a T-shaped subassemblage was isolated from the inflection points of the beam and the column of a moment-resisting frame subjected to a seismic lateral load.

Table 2
Test results and failure modes [11,12]

Specimen	Interstory drift angle (% rad)	Total plastic rotation (% rad)	Failure mode
SRL20	5.06	4.37	Rib fracturing at the plastic hinge location
SRL30	4.59	4.11	Lateral torsional buckling; minor crack in the weld between rib and beam flange
SRE6-1	4.84	4.05	Rib fracturing at the plastic hinge location
SRE6-2	4.84	4.04	Beam flange fracturing at the rib tip
SRE7-1	4.37	3.15	No connection failure; only minor crack in the weld between rib and beam flange
SRE7-2	4.37	3.27	Fracturing of rib and beam flange at the beam–column interface

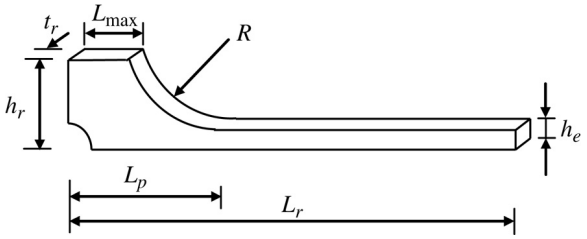

Fig. 2. Geometry of lengthened rib.

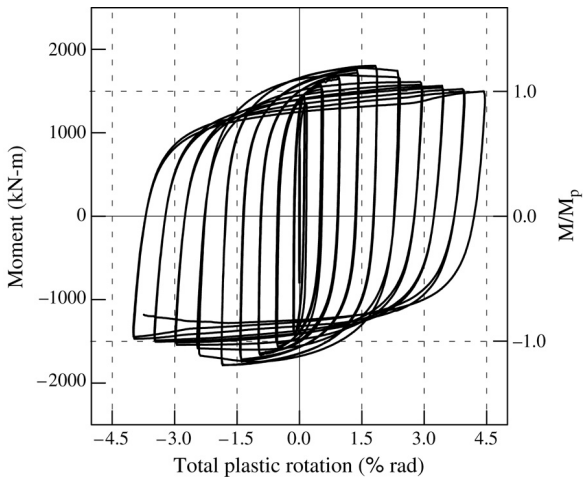

Fig. 3. Moment versus plastic rotation relationship of specimen SRE6-1 [12].

Moreover, incremental increase displacement was applied to represent the cyclic load. A predetermined loading history, following the loading protocol [13], was imposed at the end of the cantilever beam.

All the specimens behaved in a similar ductile manner. The beam section displayed intensive yielding. Ductile behavior was guaranteed by forming a plastic hinge at the specified location. Table 2 lists the test results and failure modes. The specimens could sustain a story drift angle of at least 4% rad. All the specimens developed reliable plastic rotation greater than 3% rad, which was primarily contributed by beam yielding. Fig. 3 shows typical loops of moment versus plastic rotation. Hysteretic curves demonstrated that specimens had stable energy dissipation capacity under cyclic loading. Slight strength degradation

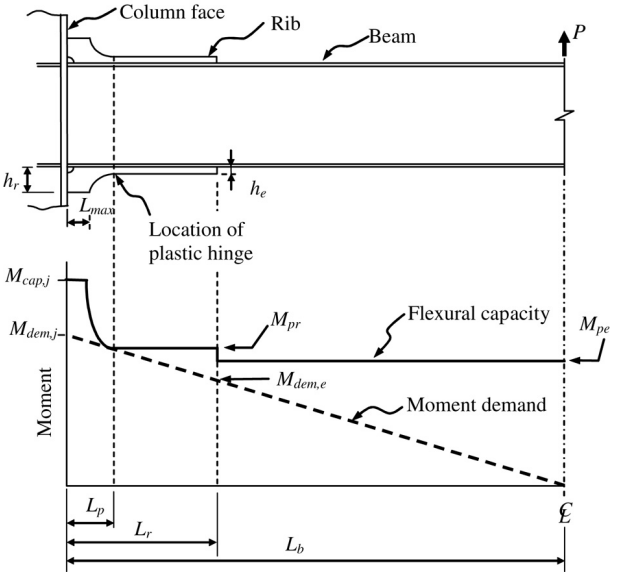

Fig. 4. Plastic hinge formation of lengthened rib connection.

observed on the hysteretic curves of several specimens resulted from local buckling of the beam. The maximum flexural moment of the connections developed at a story drift angle of 4% rad exceeded the nominal plastic flexural capacity of the beam. Furthermore, failure modes, as listed in Table 2, differed among specimens depending on the size of the lengthened rib. The failure modes included the fracture on the groove weld joining the rib and the column flange, the fracture of the beam flange at the rib tip, and the propagating crack on the rib.

3. Parametric study

3.1. Geometrical parameters of lengthened rib

A parametric analysis was performed to examine the effects of rib design variables on the connection behavior owing to only a limited number of tests being conducted. Test results have shown that seismic behavior and the failure mode of rib-reinforced connections are mainly dependent on the reinforcing rib. The flexural capacity of the beam is considered for determining the effect of the rib design variables on the connection behavior. Fig. 4 illustrates the

relationship between the flexural capacity and moment demand of a beam subjected to seismic force. The effect of gravity loads on the moment demand distribution is neglected assuming that the moment caused by gravity loads is small compared to that caused by seismic force. A more specific curved moment diagram should be considered if the gravity loads are extremely large. Plastic hinging of the beam is assumed to occur at the intersection of lines of flexural capacity and moment demand, which is located at some distance from the column face. The most important geometric aspects of the lengthened rib are the cross section of the main reinforced part and the extension, and the rib length. Accordingly, three geometrical parameters are defined for configuring the rib plate.

First, a parameter ρ is used to determine the plastic flexural capacity at the location of the plastic hinge, M_{pr}:

$$M_{pr} = \rho M_{pe} \tag{1}$$

where

$$M_{pe} = Z_b R_y F_y. \tag{2}$$

M_{pe} denotes the flexural capacity of the beam section, which can be calculated using the expected yield strength $R_y F_y$; R_y is a multiplier accounting for expected material overstrength, in accordance with AISC Seismic Provisions for Structural Steel Buildings [14]; Z_b represents the plastic section modulus of the beam; and F_y is the specified minimum yield strength of the steel. The value of ρ relates to the amount of reinforcement of the rib extension, and is defined as an extension reinforcement factor. Furthermore, larger ρ results in higher beam flexural capacity at the location of the plastic hinge. On the basis of the flexural capacity at the location of the plastic hinge, M_{pr}, the cross section of the rib extension can be determined by calculating the plastic section moduli of the beam and the rib extension.

Second, a parameter α is used to determine the flexural capacity at the beam-to-column interface, $M_{\text{cap},j}$:

$$M_{\text{cap},j} = \alpha M_{\text{dem},j} \tag{3}$$

where $M_{\text{dem},j}$ denotes the moment demand at the beam-to-column interface, which can be calculated as follows:

$$M_{\text{dem},j} = \frac{L_b}{L_b - L_p} M_{pr} \tag{4}$$

where L_b represents the length of the half span of the beam and L_p is the distance from the column face to the plastic hinge location. As indicated in Eq. (3), the parameter α denotes the ratio of moment capacity to demand at the beam-to-column interface, and is defined as a main reinforcement factor of the rib. Furthermore, α should exceed 1.0 to ensure sufficient margin of safety at the beam-to-column interface. Consequently, the cross section of the main reinforced part of the rib can be determined on the basis of the flexural capacity $M_{\text{cap},j}$.

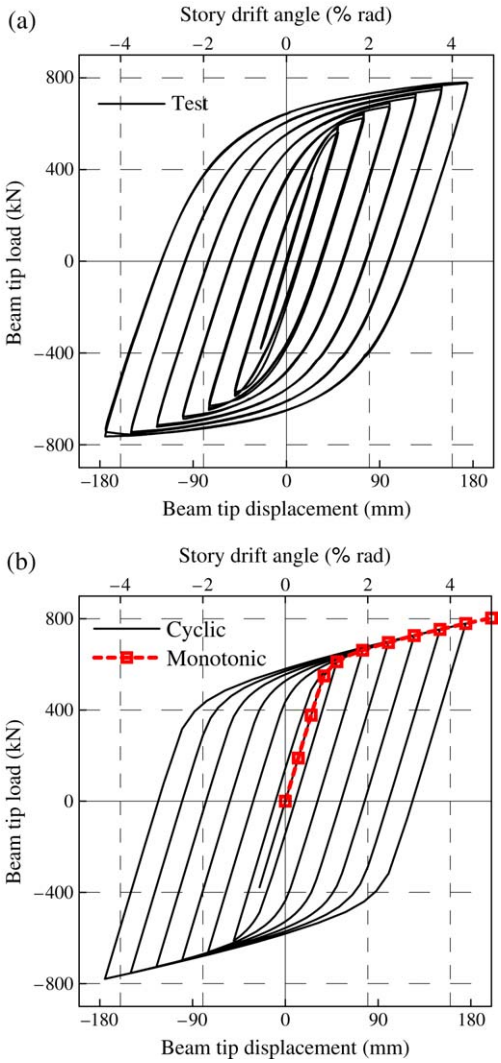

Fig. 5. Verification of hysteresis curves: (a) experiment; (b) finite element analysis.

Third, a parameter γ is used to determine the overall rib length, L_r, on the basis of the following equations:

$$\gamma = \frac{M_{pe}}{M_{\text{dem},e}} \tag{5}$$

and

$$M_{\text{dem},e} = \frac{L_b - L_r}{L_b - L_p} M_{pr} \tag{6}$$

where $M_{\text{dem},e}$ denotes the flexural demand at the tip of the rib extension. The parameter γ represents a factor that determines the rib length. Higher γ results in a longer rib and higher margin of safety at the rib tip.

3.2. Finite element modeling and validation

The parametric study was conducted using the finite element analysis to study the behavior of seven connections. An unreinforced connection was modeled to represent the

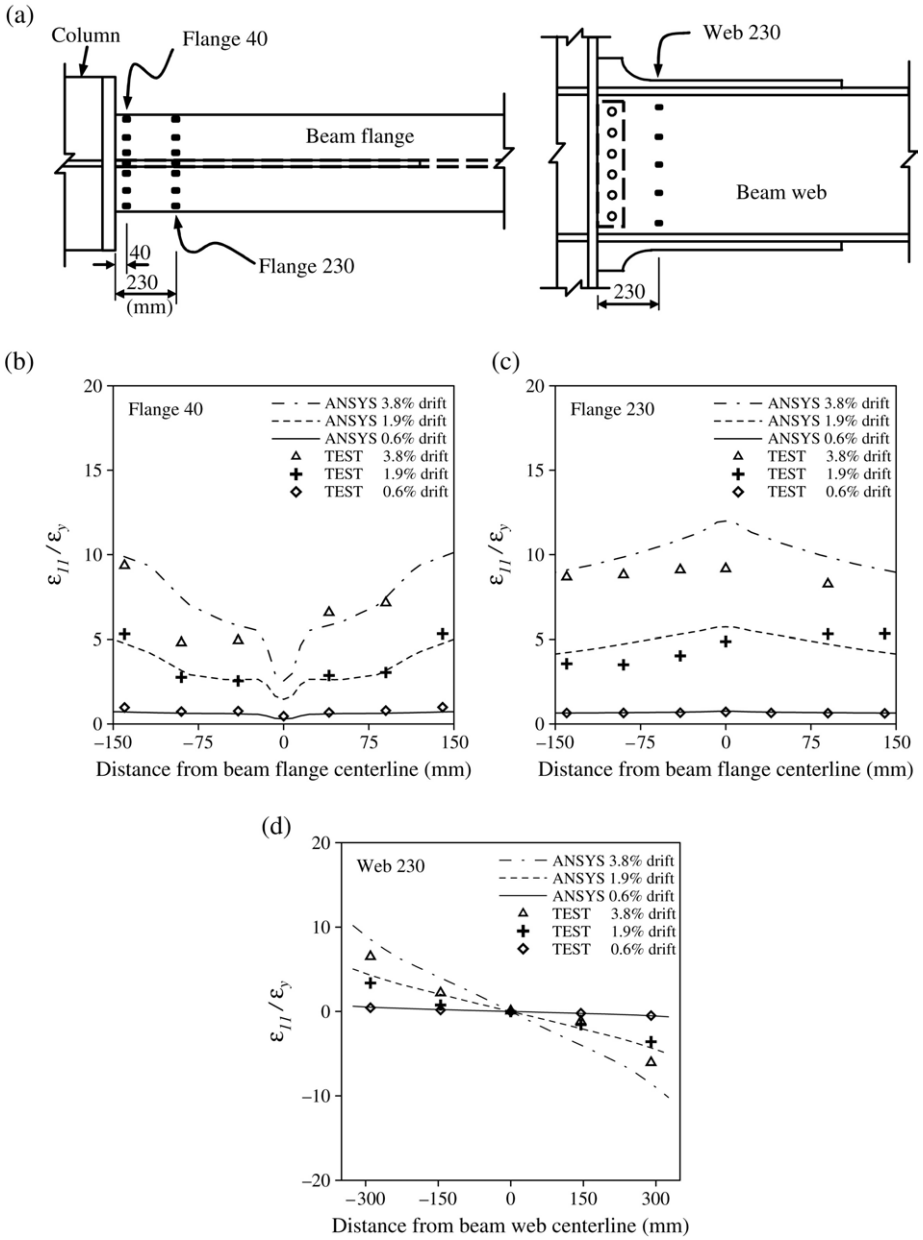

Fig. 6. Verification of longitudinal strain distribution: (a) strain gauge location; (b) on beam flange 40 mm away from column face; (c) on beam flange at plastic hinge location; (d) on beam web at plastic hinge location.

pre-Northridge moment connection. Additionally, six rib-reinforced connections were designed to reflect three design parameters of the lengthened rib. A control model of rib-reinforced connection employed parameters $\alpha = 1.10$, $\rho = 1.05$ and $\gamma = 1.10$. The other five rib-reinforced connections changed one parameter at a time from among parameters $\alpha = 1.05$ and 1.15, $\rho = 1.10$, and $\gamma = 1.05$ and 1.15 while keeping the remaining parameters constant. The rib used in the control model of rib-reinforced connection was 19 mm thick, 107 mm high, and 580 mm long, with a 19 mm high extension. The other ribs used in the models had dimensions ranging from 19×19 to 27×27 mm for the cross section of the rib extension, 90–123 mm high for the main reinforced part, and 460–690 mm in length.

This study used the finite element analysis program ANSYS [15] for model analysis. Each model consisted of an H-shaped H588 × 300 × 12 × 20 beam and an H550 × 550 × 30 × 40 column, assuming the ASTM A572 Grade 50 steel. Further modeling for materials can be found in Ref. [11].

The numerical results were compared with the experimental results for both global and local responses to validate the accuracy of the finite element modeling. Global behavior is presented in terms of hysteretic loops. Fig. 5 presents both the numerical and the experimental hysteresis curves of the beam tip load versus the corresponding displacement for

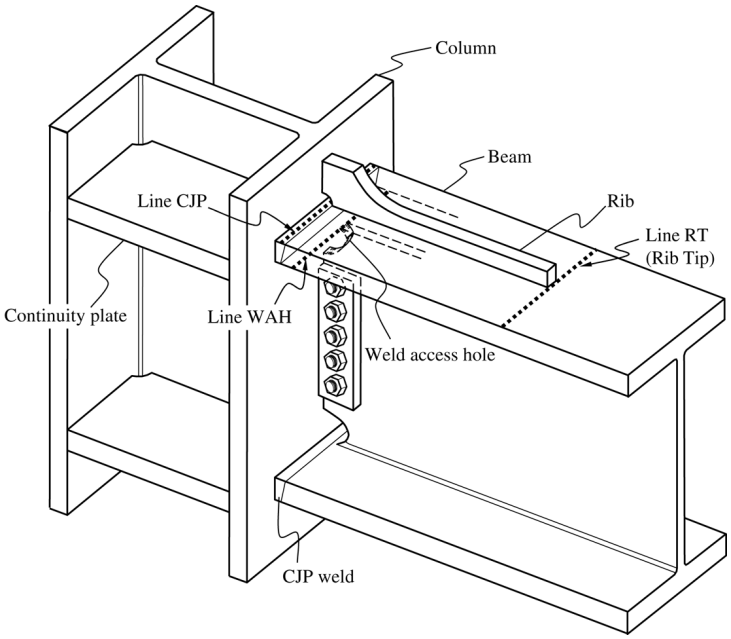

Fig. 7. Critical sections.

specimen SRE7-1 [12]. Good correlation between the numerical and the experimental work was obtained. The stiffness and the ultimate load at each cycle can be reasonably simulated up to a story drift angle of 4% rad, except that the experimental curves are smoother and wider at yield than the numerical ones. Moreover, as shown in Fig. 5(b), the numerical results of a monotonic loading are also presented with those obtained cyclically. The monotonic results can correlate well with the envelope of the cyclic force–displacement curve.

The verification of the local behavior was performed by comparing the strain distributions at the locations concerned. Fig. 6 shows the normalized longitudinal strain distribution on the beam flange and the web at the story drift angles of 0.6%, 1.9%, and 3.8% rad. A reasonable agreement between the numerical results and the physical tests was generally achieved. On the basis of the satisfactory performance, the finite element modeling with monotonic loading was used to proceed with the parametric study.

3.3. Analysis results

The stress and strain distributions in three critical sections of the connection were studied. The selection of critical sections was based on the fracturing location in pre-Northridge moment connections. Fig. 7 shows the critical sections, presented by lines running across the width of the beam flange. Line CJP is located at the complete joint penetration (CJP) groove weld joining the beam and column flanges because many fractures have been found at this groove weld during the Northridge earthquake. Line WAH is located at the root of the weld access hole (WAH), from which the beam flange fractured, as shown by the pre-Northridge connections [3,4,16]. Finally, line RT is located at the rib tip because stress concentration in the beam flange in this region caused fracturing of the beam flange, as demonstrated from the triangular rib-reinforced connections [4,9].

The stress distribution and strain demand in the connection were demonstrated using two significant indicators, normalized longitudinal stress and PEEQ index. The normalized longitudinal stress is defined as the normal stress σ_{11}, along the longitudinal axis of the beam, normalized by the yield stress F_y. Meanwhile, the PEEQ index, which represents local strain demand, is defined as the plastic equivalent strain (PEEQ) divided by the yield strain ε_y.

The distributions of normalized longitudinal stresses and PEEQ indices along lines CJP and WAH are shown in Figs. 8 and 9, respectively. The longitudinal stress was considered at a story drift angle of 0.5% rad to evaluate the connection behavior within an elastic range, because many pre-Northridge connections failed prematurely at limiting plastic rotation. The other indicator, the PEEQ index, was used to assess the connection behavior under high strain at a story drift angle of 4.0% rad. The unreinforced connection demonstrated stress concentration and highly localized plastic strain demand in the middle of the beam flange, especially at the root of the weld access hole. Evidently, the rib-reinforced connection effectively reduced the stress distribution and strain demand at the CJP weld and WAH region, during both the elastic and inelastic stages. With the introduction of the rib, the maximum PEEQ index at the toe of the weld access hole was considerably reduced from 21.2 to 9.6, a reduction of 55%. The inherent concentrations of stress and strain of the unreinforced connection were significantly reduced by the presence of the lengthened rib

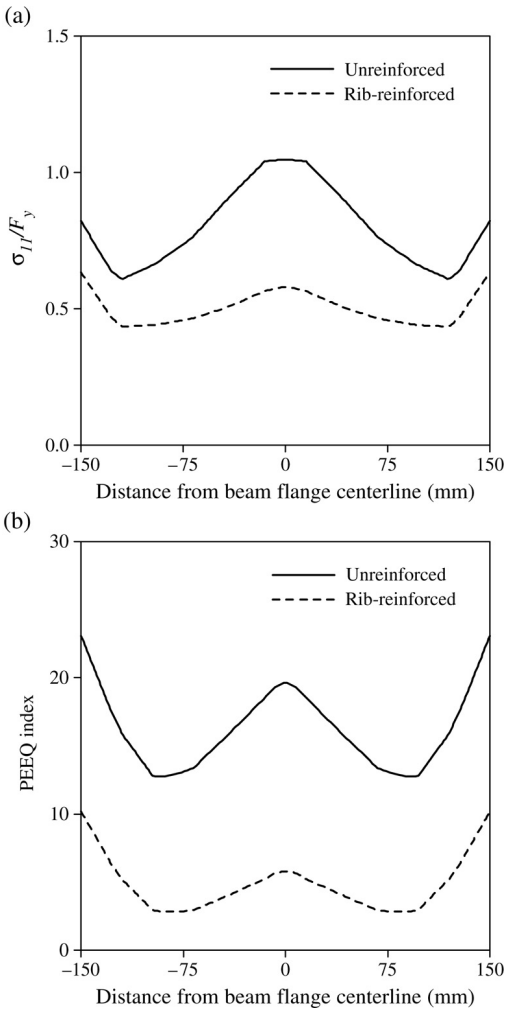

Fig. 8. Distribution of normalized longitudinal stresses and PEEQ indices along line CJP: (a) at 0.5% story drift angle; (b) at 4.0% story drift angle.

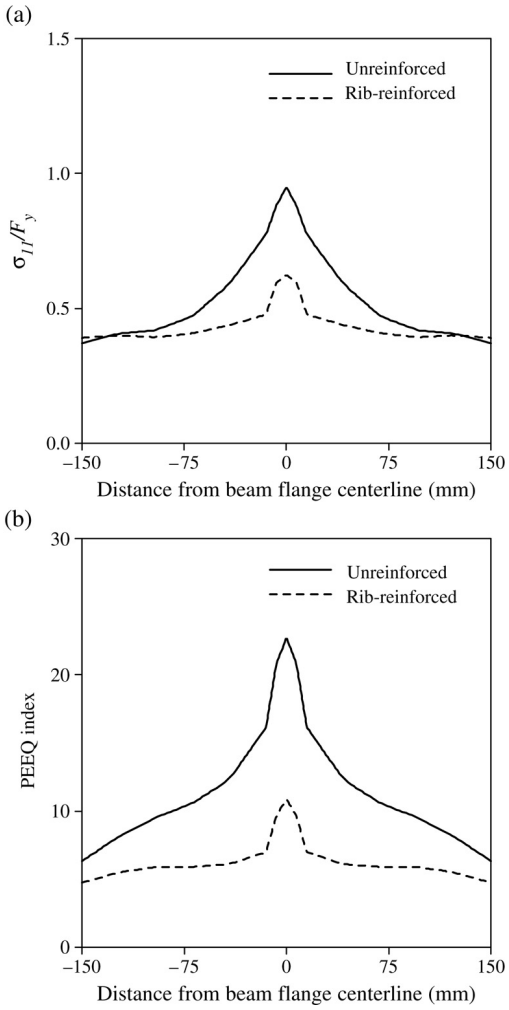

Fig. 9. Distribution of normalized longitudinal stresses and PEEQ indices along line WAH: (a) at 0.5% story drift angle; (b) at 4.0% story drift angle.

at the centerline of the beam flange. The potential for brittle failure in the weld access hole region thus was diminished.

3.4. Effects of design parameters

To assess the influences of the rib on the distributions of stresses and strains in the critical sections, the maximum normalized longitudinal stress and PEEQ index along the lines were captured for comparison. Fig. 10 shows a comparison between the results of the unreinforced and rib-reinforced connections for different values of α, along lines CJP and WAH, at story drift angles of 0.5% and 4% rad. Since it is the main reinforcement factor, the value of α affects the cross section of the main reinforced part of the rib. At line CJP, the maximum normalized longitudinal stresses of rib-reinforced connections with α of 1.05, 1.10, and 1.15 were decreased by 40%, 44%, and 47%, respectively, compared to those of the unreinforced connection and also were reduced by 28%, 35%, and 38% at line WAH. Fig. 10(b) shows further reduction of plastic strain demand. These figures indicate that the stress and strain demands at the critical sections of lines CJP and WAH can be significantly reduced by the rib. Nevertheless, the effectiveness of the rib in reducing the maximum stress and plastic strain reduced with increasing α. It is reasonable to use $\alpha = 1.10$ for design purposes.

Fig. 11 shows the effects of ρ values of 1.05 and 1.10 on the normalized longitudinal stress and plastic strain demand in the critical sections. Different values of ρ lead to different cross sections of the rib extension. Although parameters α and γ remained unchanged, a larger cross section of the main reinforced part of the rib was required owing to the increase of ρ. Therefore, increasing the parameter ρ reduces the stress and strain demands, especially in the PEEQ index. Reductions of 71% in line CJP and 52% in line WAH, compared to the unreinforced connection, were noted in the PEEQ index of the model with $\rho = 1.05$. The model with $\rho = 1.05$ achieves significant improvement, while parameter $\rho = 1.10$ results in smaller stress and PEEQ index values.

Fig. 12 shows the effects of the parameter γ on normalized longitudinal stress and PEEQ index at lines CJP, WAH, and RT. The value of γ affects the rib length. Three

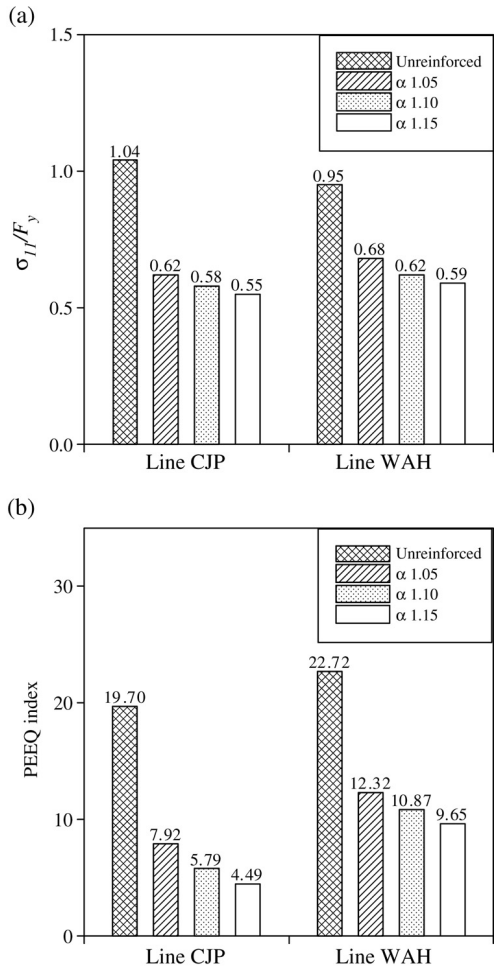

Fig. 10. Comparison of results of different values of α: (a) normalized longitudinal stresses at 0.5% story drift angle; (b) PEEQ indices at 4% story drift angle.

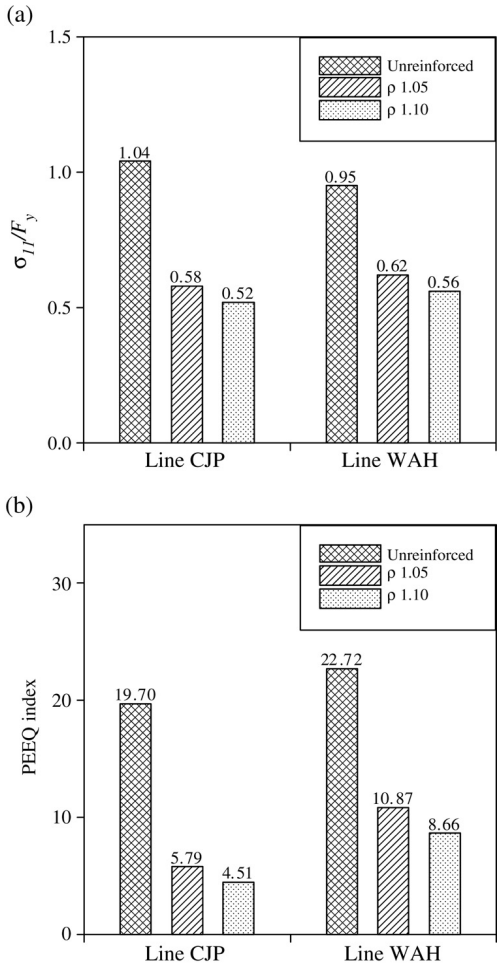

Fig. 11. Comparison of results of different values of ρ: (a) normalized longitudinal stresses at 0.5% story drift angle; (b) PEEQ indices at 4% story drift angle.

values of the parameter γ, 1.05, 1.10, and 1.15, were used for the models, and the corresponding rib lengths were 460 mm, 580 mm, and 690 mm, respectively. The figure demonstrates that different values of γ exerted negligible effects on lines CJP and WAH because the value of γ altered only the rib length. The longitudinal stresses of the rib-reinforced connections at line RT were only slightly higher than those of the unreinforced connection. Moreover, the longitudinal stress is insensitive to the variation of the parameter γ. Nevertheless, increasing the value of the parameter γ constantly leads to a decrease in the value of the PEEQ index.

4. Design considerations

4.1. Determination of design parameters

The geometrical parameters of the rib are determined on the basis of the results of the experiment and finite element analysis. Table 3 lists the values of three parameters used for designing the ribs used in the specimens. Specimen SRE6-2 was designed to have the smallest γ, while specimen SRE7-2 had the smallest ρ.

Table 3
Values of parameters used in specimens

Specimen	Parameter		
	α	ρ	γ
SRL20	1.17	1.05	1.22
SRL30	1.22	1.12	1.15
SRE6-1	1.10	1.05	1.15
SRE6-2	1.05	1.05	1.05
SRE7-1	1.05	1.05	1.10
SRE7-2	1.05	1.03	1.10

Because the parameter α, the main reinforcement factor, provides the margin of safety at the beam-to-column interface, design safety increases with α. A larger value of α requires a larger cross section of the main reinforced part. Consequently, a thicker and taller rib becomes necessary.

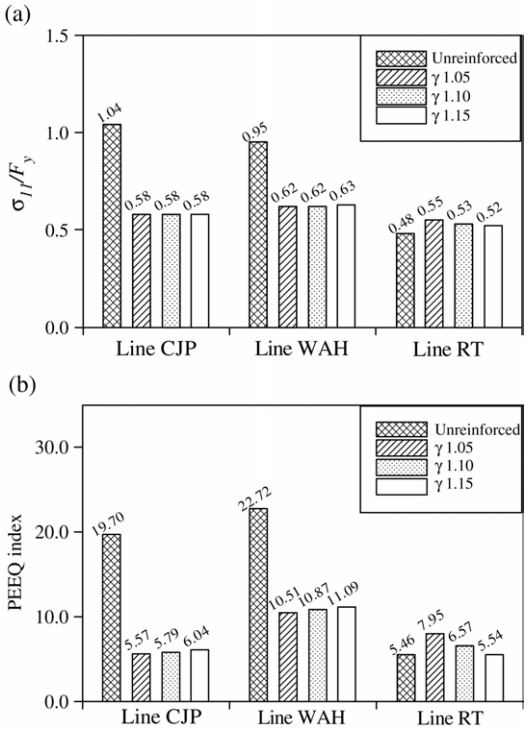

Fig. 12. Comparison of results of different values of γ: (a) normalized longitudinal stresses at 0.5% story drift angle; (b) PEEQ indices at 4% story drift angle.

Furthermore, none of the specimens failed at the beam-to-column interface except specimen SRE7-2. For design purposes, the parameter α is conservatively set to 1.10 or greater to avoid the brittle failure mode occurring at the beam-to-column interface. This study also suggests that the height of the main reinforced part should not exceed the slab thickness, which is generally less than 150 mm.

The parameter ρ, the extension reinforcement factor, directly influences the cross section of the rib extension. A high value of ρ is not suitable for the formation of the plastic hinge in the beam, as observed from specimen SRL30, that displayed lateral buckling of the beam at the rib tip. As demonstrated by the finite element analysis, the distributions of stresses and strains of the rib-reinforced connection are not very sensitive to the variation of parameter ρ. Although rib fracturing eventually occurred in most of the specimens, $\rho = 1.05$ leads to acceptable behavior.

The difference between flexural capacity and moment demand at the rib tip becomes small with reducing γ. That is, given small γ the potential of the stress concentration occurring in the beam flange increases. For example, specimen SRE6-2 was designed to have minimum rib extension with $\gamma = 1.05$, and specimen SRE6-2 failed because of the cracking and eventual fracturing of the beam flange at the rib tip. The remaining specimens with γ of 1.10 or more did not suffer this kind of failure. Therefore, $\gamma = 1.10$ is suggested as a minimum; however, economic concerns mean that γ should not be too large.

4.2. Recommended design procedure

On the basis of the parametric study and experimental results, parameters of $\alpha = 1.10$, $\rho = 1.05$, and $\gamma = 1.10$ can be used reliably for design purposes. The design procedure for a lengthened rib-reinforced connection is summarized as follows.

1. Compute the expected plastic flexural capacity of the beam, M_{pe}, using Eq. (2).
2. Calculate the design flexural capacity at the location of the plastic hinge, M_{pr}, by selecting a minimum value of $\rho = 1.05$ and using Eq. (1).
3. Select a cross section, $t_r \times h_e$, of the rib extension on the basis of M_{pr}.
4. Assume the location of the plastic hinge by setting L_p as the larger of $d_b/3$ and 200 mm, where d_b is the beam depth.
5. Use Eqs. (3) and (4) to obtain the design flexural capacity at the beam-to-column interface, $M_{\text{cap},j}$, setting $\alpha = 1.10$.
6. Determine the height of the main reinforced part of the rib, h_r, on the basis of $M_{\text{cap},j}$.
7. Calculate the rib length, L_r, from Eqs. (5) and (6) by assuming a minimum value of $\gamma = 1.10$.
8. Select $L_{\max}$ as the larger of $L_p/3$ and 80 mm, and set the radius of the curved part to equal L_p.

Furthermore, a strong column–weak beam criterion should be checked for the rib-reinforced connection because the welded rib increases the flexural strength of the beam.

5. Conclusion

The following conclusions are obtained on the basis of the results of the parametric study conducted via finite element analysis. Analysis results demonstrate that a single lengthened rib can be used to reduce the stress concentration and plastic strain demand in the beam flange groove weld and the weld access hole region, and to diminish the fracture potential of the beam flange at the beam-to-column interface. The numerical results for the rib-reinforced connection revealed that extensive yielding occurs in the beam away from the column face, and the plastic hinge reliably forms in the beam. Moreover, the rib extension can effectively eliminate the localized high stress that occurs in the beam flange at the rib tip. On the basis of the effects of three geometrical parameters of the lengthened rib on the stress and strain distributions, this study suggests parameters and confirms them with the test results. The parametric study showed that the parameters of extension reinforcement factor $\rho = 1.05$, main reinforcement factor $\alpha = 1.10$, and rib length factor $\gamma = 1.10$ are reasonable for use in rib design.

Acknowledgement

The authors acknowledge the support from the Sinotech Engineering Consultants, Inc., for this research program.

References

[1] Youssef NFG, Bonowitz D, Gross JL. A survey of steel moment-resisting frame buildings affected by the 1994 Northridge earthquake. Report No. NISTIR 5625, National Institute of Standards and Technology; 1995.

[2] Lu LW, Ricles JM, Mao C, Fisher JW. Critical issues in achieving ductile behaviour of welded moment connections. Journal of Constructional Steel Research 2000;55:325–41.

[3] Stojadinovic B, Goel SC, Lee KH, Margarian AG, Choi JH. Parametric tests on unreinforced steel moment connections. Journal of Structural Engineering, ASCE 2000;126(1):40–9.

[4] Chen CC, Chen SW, Chung MD, Lin MC. Cyclic behaviour of unreinforced and rib-reinforced moment connections. Journal of Constructional Steel Research 2005;61(1):1–21.

[5] AISC. Seismic provisions for structural steel buildings. Chicago (IL): American Institute of Steel Construction; 1997.

[6] Ricles JM, Mao C, Lu LW, Fisher JW. Inelastic cyclic testing of welded unreinforced moment connections. Journal of Structural Engineering, ASCE 2002;128(4):429–40.

[7] FEMA. Recommended seismic design criteria for new steel moment-frame buildings. Report No. FEMA-350, Federal Emergency Management Agency; 2000.

[8] Popov EP, Tsai KC. Performance of large seismic steel moment connections under cyclic loads. Engineering Journal, AISC 1989; 26(2):51–60.

[9] Engelhardt MD, Sabol TA, Aboutaha RS, Frank KH. Testing connections. Modern Steel Construction, AISC 1995;35(5): 36–44.

[10] Anderson JC, Duan X. Repair/upgrade procedures for welded beam to column connections. Report no. PEER 98/03, Richmond (CA): Pacific Earthquake Engineering Research Center; 1998.

[11] Chen CC, Lee JM, Lin MC. Behaviour of steel moment connections with a single flange rib. Engineering Structures 2003;25:1419–28.

[12] Chen CC, Lu CA. Cyclic behavior of steel moment connections strengthened by flange rib. In: Proceedings of the 5th Korea–Taiwan–Japan joint seminar on earthquake engineering for building structures; 2003. p. 71–9.

[13] ATC. Guidelines for seismic testing of components of steel structures. Report ATC-24, Redwood City (CA): Applied Technology Council; 1992.

[14] AISC. Seismic provisions for structural steel buildings. Chicago (IL): American Institute of Steel Construction; 2002.

[15] ANSYS User Manual. ANSYS, Inc.; 2001.

[16] Miller DK. Lessons learned from the Northridge earthquake. Engineering Structures 1998;20(4–6):249–60.